JACS
JOURNAL OF THE AMERICAN CHEMICAL SOCIETY

Communication

pubs.acs.org/JACS

Facile and Efficient Preparation of Anisotropic DNA-Functionalized Gold Nanoparticles and Their Regioselective Assembly

Li Huey Tan,[†] Hang Xing,[†] Hongyu Chen,[‡] and Yi Lu*[,†]

[†]Department of Chemistry, University of Illinois at Urbana—Champaign, Urbana, Illinois 61801, United States
[‡]Division of Chemistry & Biological Chemistry, Nanyang Technological University, Singapore 637371

Supporting Information

ABSTRACT: Anisotropic nanoparticles can provide considerable opportunities for assembly of nanomaterials with unique structures and properties. However, most reported anisotropic nanoparticles are either difficult to prepare or to functionalize. Here we report a facile one-step solution-based method to prepare anisotropic DNA-functionalized gold nanoparticles (a-DNA-AuNP) with 96% yield and with high DNA density (120 ± 20 strands on the gold hemisphere). The method is based on the competition between a thiolated hydrophilic DNA and a thiolated hydrophobic phospholipid and has been applied to prepare a-DNA-AuNPs of different sizes and with a variety of DNA sequences. In addition, DNA strands on the a-DNA-AuNPs can be exchanged with other DNA strands with a different sequence. The anisotropic nature of the a-DNA-AuNPs allows regioselective hetero- and homonuclear assembly with high monodispersity, as well as regioselective functionalization of two different DNA strands for more diverse applications.

DNA-functionalized gold nanoparticles (DNA-AuNPs) are among the most useful building blocks for nanoscale assembly of a variety structures,[1] mainly due to the programmable nature of the DNA strands that allow structural tuning and introduction of functional groups not achievable by conventional methods.[2] Most DNA-AuNPs used in assembly, however, are isotropic particles. Because of the unique directional interactions imparted by anisotropic DNA-functionalized gold nanoparticles (a-DNA-AuNPs), such as Janus particles[3] and regioselective assembled systems with nanorods and nanospheres,[4] these a-DNA-AuNPs have been demonstrated to form more diverse structures with unique properties,[5] including chiral metamaterials with promising applications as circular polarizers,[6] negative refractive index materials,[7] chiral plasmonic rulers.[8] and chiral-selective sensors.[9] Despite such promise, a-DNA-AuNPs are challenging to synthesize,[10] with only a few efficient methods,[11] as most synthesis methods require careful surface-based fabrication, long incubation time, or have low yields that require additional step of purification.[5a,b,12] Furthermore, the prepared anisotropic nanoparticles are often difficult to functionalize selectively.[13] Here, we report a facile method to synthesize a-DNA-AuNPs with high yields, and subsequently functionalized with DNA for chemoselective and regioselective assembly of a variety of AuNPs. We further demonstrate that this particle can be used to regioselectively functionalize two different DNA strands on the same particle.

An anisotropic AuNP (a-AuNP) was synthesized based on competition between hydrophobic and hydrophilic ligands on gold nanoparticle surface to produce anisotropic attachment of polymers, as reported previously.[13,14] While this method allows facile synthesis of a-AuNPs in high yield, the a-AuNPs have not been used for nanoscale assembly, due to limited functional groups that can be used for the synthesis and low efficiency for post-synthesis modifications. Initial functionalization attempts in mixing a AuNP with thiolated DNA failed, probably due to the high density of the small thiolated ligands already present on the Au surface and low thiolated ligand exchange rate, as observed previously.[13] To overcome this limitation, we used a 10-mer oligo of adenine with thiol at the 5′ end (HS-A10) as the hydrophilic ligand and a thiolated phospholipid (PSH) as the hydrophobic ligand (Figure 1a). Both ligands were incubated with either 15 or 20 nm AuNPs and an amphiphilic polymer polystyrene-*b*-poly(acrylic acid) (PSPAA) in DMF/H_2O at 95 °C for 2 h, and the mixtures were then cooled to room temperature. Transmission electron microscope (TEM) images of the samples containing 15 nm (Figure 1b, large-area view in Figure S1) or 20 nm AuNPs (Figure 1c and Figure S2) shows that a-DNA-AuNPs were formed uniformly throughout, suggesting that this method can be applied for synthesis of a-DNA-AuNPs of different sizes. To quantify the synthesis yield, we counted a total of 633 particles from the TEM micrographs and found ∼96% of 20 nm a-DNA-AuNPs, with the remaining 4% having either no polymer attachment, full polymer encapsulation or encapsulated dimer of particles.

The ratio of PSH to DNA can be tuned to balance the competition between the two ligands. As shown in Figure S3, a PSH to DNA ratio of 2 gave a larger polymer but still uniform coverage on the AuNP, while a 1:1 ratio resulted in a mixture of unencapsulated and partially encapsulated particles (Figure S4). A ratio of 1:2.8 and 1:1.5 was found to be optimal for 15 and 20 nm a-DNA-AuNPs, respectively. Control experiments using only DNA or only PSH as the ligand resulted in unencapsulated AuNPs (Figure 1d) and the fully encapsulated AuNPs with PSPAA (Figure 1e), respectively. These results support the roles of DNA as a hydrophilic ligand and PSH as a hydrophobic ligand. The areas on the AuNPs not encapsulated by polymer are covered by DNA.

Received: August 3, 2013
Published: October 22, 2013

dx.doi.org/10.1021/ja408033e | *J. Am. Chem. Soc.* 2013, 135, 17675−17678

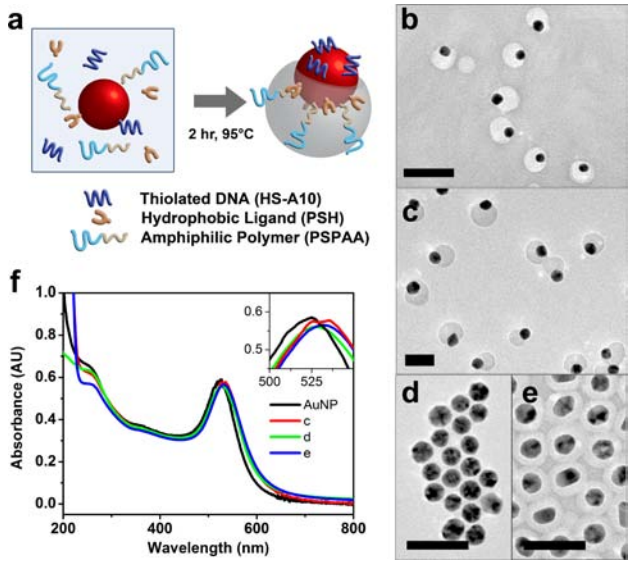

Figure 1. (a) Synthesis of a-DNA-AuNP, where HS-A10, PSH, PSPAA, and AuNPs are incubated at 95 °C for 2 h in DMF/H_2O. TEM micrographs of (b) 15 nm a-DNA-AuNP, (c) 20 nm a-AuNP, (d) completely unencapsulated AuNP when no PSH was added, (e) fully encapsulated AuNP when no SH-A10 was added. (f) UV−Vis absorption spectra of citrate-capped AuNP, a-DNA-AuNP sample in (b), and fully encapsulated AuNP (d); inset shows the shift of the plasmon peak from 525 to 535 nm. Scale bar = 50 nm.

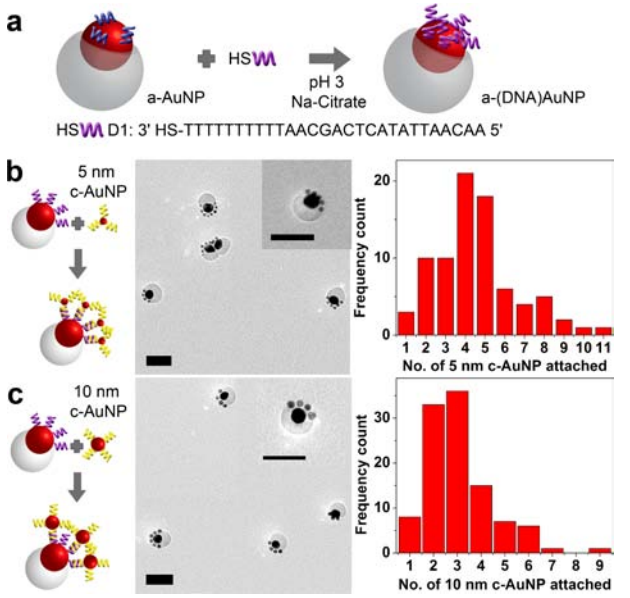

Figure 2. (a) Functionalization of a-AuNP with D1 resulting in a-(D1)-AuNP. Schematic of selective assembly of a-(D1)-AuNP with (b) 5 nm c-AuNPs and (c) 10 nm c-AuNPs with its corresponding TEM micrographs and histogram showing particle analysis. Scale bars = 50 nm.

To investigate whether this method can be generally applied to DNA strands with different sequences, thiolated A10, A30, and R20 (full sequence available in SI) were used to repeat the above procedures, and all of them produced anisotropic structures, as long as proper PSH to DNA ligand ratios of 1.5, 2.2, and 5.6 are maintained, respectively (Figures S2, S5, and S6). These results suggest that DNA sequences have minimal effects on the formation of an anisotropic structure. Instead, the ligand ratio is critical, especially to produce uniform anisotropic encapsulation of AuNPs.

Localized surface plasmon resonance spectra of AuNPs are strongly correlated to the structure of the AuNP and its monodispersity. The UV−Vis absorbance spectra of the a-DNA-AuNPs showed a clear peak at 535 nm, which is slightly red-shifted from that of citrate-capped AuNPs (Figure 1f). The peak width was retained, and there were no additional peaks or shoulders, suggesting that the AuNPs are well-dispersed and individually modified with polymer after synthesis, which is consistent with the TEM results in Figure 1c. The slight red shift of the plasmon resonance of the a-DNA-AuNP is due to the functionalization of the AuNP with a ligand shell.

Upon demonstrating the one-pot synthesis of these a-DNA-AuNPs, we next investigated regioselective ligand exchange on the a-DNA-AuNPs to introduce any desired functionality at specific locations. To achieve this goal, we adopted a quick functionalization method[15] where thiolated DNA (D1) was incubated with a-DNA-AuNPs in 50 mM of pH 3 Na-citrate and NaCl solution to give a-(D1)-AuNPs (Figure 2a). The UV−Vis absorption spectra of a-DNA-AuNPs before and after functionalization with D1 were nearly identical, indicating that the functionalization process did not disrupt the integrity of the a-DNA-AuNP particle (Figure S7). The DNA attachment was confirmed by functionalizing the a-DNA-AuNP with fluorescein (FAM)-labeled DNA at the 5′ end. From the fluorescence measurement, we found that ∼120 ± 20 strands of DNA were functionalized per particle and 100 ± 20 complementary DNA strands can be attached per particle (Figure S8 and Table S1). Control experiments using nonthiolated DNA strands indicated a negligible amount of DNA (0.3 strands attached per particle; data in Table S1) was detectable, suggesting that the attachment of DNA was via the thiol−gold interaction, and there were little nonspecific binding of DNA to the polymer layer. In comparison to the maximum loading of 180 ± 20 DNA strands on an isotropically functionalized spherical 20 nm AuNP,[16] the DNA density on the a-DNA-AuNP is comparable considering that only half of the a-AuNP surface was available for functionalization. Such high-density has been shown to increase AuNP stability and allow cooperative assembly.[17]

To probe regioselective functionalization of D1 on the a-(D1)-AuNP, 5 nm AuNPs functionalized with complementary sequence to D1 (c-AuNPs) were used to probe the hybridization ability and position of the DNA. After removing excess 5 nm c-AuNPs via centrifugation, TEM images showed that the 5 nm c-AuNPs attached only onto the exposed AuNP region and not on the polymer shell (Figures 2b and S9), indicating that the D1 on a-(D1)-AuNP not only retained its hybridization ability but also its regioselectivity. When 5 nm AuNPs with noncomplementary strands were used, no significant attachment of 5 nm AuNPs on a-(D1)-AuNP was observed (Figure S10). These results indicate that a-(D1)-AuNP interacts and assembles with other particles via specific hybridization of DNA. Since the interaction is sequence-specific, we expand the scope of asymmetric assembly with the use of AuNPs of various sizes but functionalized with the same cDNA. As an example, when the same a-DNA-AuNP was conjugated to either 5 nm (Figure 2b) or 10 nm AuNPs (Figure 2c), a cat-paw-like structure was formed. For the assembly with 5 nm c-AuNPs, an average of 5 ± 2 particles was found to be attached onto each a-AuNP, from a count of 81 particles tabulated from TEM micrographs (see histogram in Figure 2b). For 10 nm c-AuNPs, the average number was lower, at 3 ± 1

dx.doi.org/10.1021/ja408033e | J. Am. Chem. Soc. 2013, 135, 17675−17678

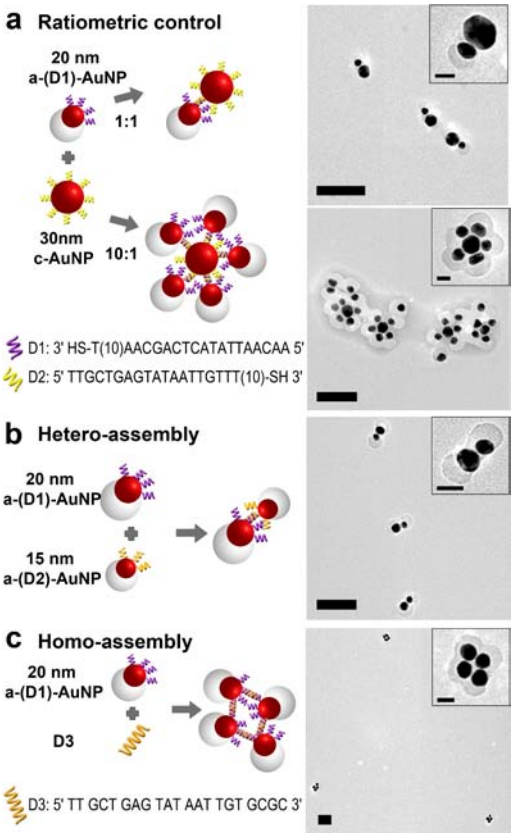

Figure 3. (a) a-(D1)-AuNP/30 nm c-AuNP assemblies at a ratio of 1:1 (top) and 10:1 (bottom). (b) Heteroassembly of 20 and 13 nm a-(D1)-AuNPs. (c) Homoassembly of a-(D1)-AuNP using linker strand D3. Scale bar = 100 nm; (insets) 25 nm.

from a total of 107 particles (see histogram in Figure 2c and large-area view in Figure S11).

Having demonstrated regioselectivity of the a-DNA-AuNPs, we further explored its application in forming more complex structures. As shown in Figures 3a and S12, when the concentration of a-DNA-AuNP is the same as that of c-AuNP, a 1:1 interaction between a-(D1)-AuNP and 30 nm c-AuNP was achieved. In the presence of an excess of a-(D1)-AuNP to 30 nm c-AuNP (10:1) satellite assemblies were formed with multiple a-(D1)-AuNPs surrounding the 30 nm c-AuNP (Figure 3a and Figure S13). This result is in contrast to previously reported assembly using isotropic DNA-AuNPs, which often resulted in AuNP aggregates.[2d,18] The protection offered by the polymers on the a-DNA-AuNP made it possible to prepare monodispersed satellite assemblies.

To demonstrate even better control over assemblies between two particles, instead of using one anisotropic and one isotropically functionalized particle, we investigated the use of all anisotropic particles. A shown in Figure 3b and Figure S14, mixing 20 nm a-(D1)-AuNP and 13 nm a-(D2)-AuNP functionalized with D1 and D2, respectively, at a 1:1 ratio resulted in heteroassembly of dimers consisting of a 20 nm and a 13 nm a-DNA-AuNP, observed as snowman-like assemblies. Of a total of 47 assemblies observed, 85% formed dimers with the correct combination, while the remaining 15% were either dimers with the wrong orientation and combination or were trimers and tetramers.

In addition to heteroassembly using two different AuNPs, homoassembly of a-(D1)-AuNP with the use of a linker strand,

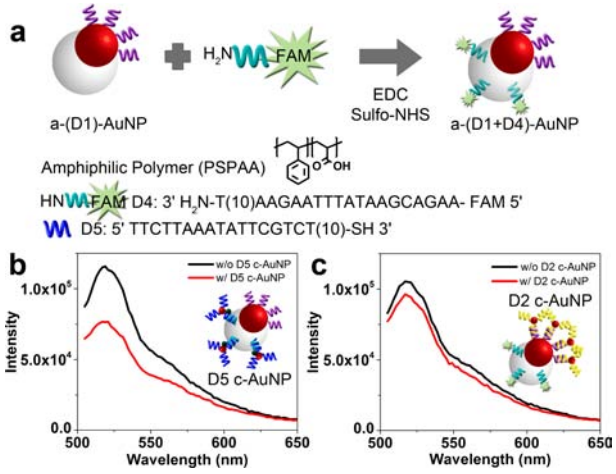

Figure 4. (a) Functionalization of D4 on the polymer side of the particle via EDC coupling. Fluorescence spectra of a-(D1+D4)-AuNP before and after incubation with (b) D5 c-AuNP and (c) D2 c-AuNP.

D3, consisting of the complementary sequence to D1, a single base spacer, and CGCG bases at the 3′ end which can self-hybridize,[1g] was investigated. Since the direction and area of interaction is controlled by the a-(D1)-AuNP, formation of Au clusters was observed (Figure 3c and Figure S15). In the absence of such directional control, as in isotropic AuNP, uncontrolled aggregations of the particles would occur.[2a]

In addition to regioselective functionalization of DNA onto the asymmetric hybrid particles and its use in selective and directional assemblies, a major advantage of the a-DNA-AuNPs is that they can provide two different functionalities with spatial separation, preventing cross-talk or interference. To achieve this goal, we introduced a second functionality through the carboxylate groups on the amphiphilic polystyrene-b-polyacrylic acid. Conjugation of the polymer, via 1-ethyl-3-(3-dimethyl-aminopropyl)carbodiimide (EDC) coupling chemistry, with amine-functionalized DNA on one end and a fluorophore (FAM) label (D4) results in formation of a-(D1+D4)-AuNP (Figure 4a). The yield of DNA coupling was calculated to be ∼30 DNA strands per particle. We then hybridized the a-(D1+D4)-AuNP to two different c-AuNPs, one functionalized with D2 that is complementary to D1 and the other with D5 that is complementary to D4. If the D1 and D4 functionalities are indeed located on different hemispheres of the particle, hybridization with D5 c-AuNP will selectively quench the fluorescence from D4 due to hybridization, while D2 c-AuNP will not quench the fluorescence from D4 becasue of lack of hybridization. Our fluorescence results in Figure 4b and c strongly support that the D1 and D4 were functionalized on the Au and polymer surface, respectively.[19]

In summary, we have demonstrated a facile method to prepare different sizes of a-DNA-AuNPs containing a variety of DNA sequences in high density. In addition, the DNA on the a-DNA-AuNP can be readily exchanged with DNA of different sequences, allowing more sequence-specific control of nanoparticle assembly. The role of DNA in this ligand competition method serves as a unique bulky ligand which allows efficient postfunctionalization on the Au surface. Taking advantage of this property, we have shown that the combination of a-DNA-AuNP and c-AuNPs results in cat-paw and satellite flower assemblies, while a-DNA-AuNPs functionalized with different DNA strands results in hetero- and homoassemblies, all with high

dx.doi.org/10.1021/ja408033e | J. Am. Chem. Soc. 2013, 135, 17675−17678

regioselectivity and monodispersity. More importantly, the anisotropic nature of our a-DNA-AuNP allows regioselective functionalization of two different DNA strands, resulting in localized quenching reactions. These a-DNA-AuNPs which are easily synthesized in high yields and versatile to be functionalized on both sides with different DNA sequences may find many applications, such as building blocks for creating optically active nanoassemblies[20] or as chiral agents for precise and specific trageting and response.[21]

■ ASSOCIATED CONTENT

Supporting Information

Experimental procedures and additional TEM images. This material is available free of charge via the Internet at http://pubs.acs.org.

■ AUTHOR INFORMATION

Corresponding Author

yi-lu@illinois.edu

Notes

The authors declare no competing financial interest.

■ ACKNOWLEDGMENTS

This work has been supported by the U.S. National Science Foundation (CMMI 0749028). L.H.T. was funded at UIUC from NIH National Cancer Institute Alliance for Nanotechnology in Cancer "Midwest Cancer Nanotechnology Training Center" Grant R25 CA154015A. TEM was carried out at the UIUC Materials Research Laboratory.

■ REFERENCES

(1) (a) Alivisatos, A. P.; Johnsson, K. P.; Peng, X.; Wilson, T. E.; Loweth, C. J.; Bruchez, M. P.; Schultz, P. G. *Nature* **1996**, *382*, 609−611. (b) Deng, Z.; Tian, Y.; Lee, S.-H.; Ribbe, A. E.; Mao, C. *Angew. Chem., Int. Ed.* **2005**, *44*, 3582−3585. (c) Aldaye, F. A.; Sleiman, H. F. *Angew. Chem., Int. Ed.* **2006**, *45*, 2204−2209. (d) Lee, J. H.; Wernette, D. P.; Yigit, M. V.; Liu, J.; Wang, Z.; Lu, Y. *Angew. Chem., Int. Ed.* **2007**, *46*, 9006−9010. (e) Nykypanchuk, D.; Maye, M. M.; van der Lelie, D.; Gang, O. *Nature* **2008**, *451*, 549−552. (f) Ding, B.; Deng, Z.; Yan, H.; Cabrini, S.; Zuckermann, R. N.; Bokor, J. *J. Am. Chem. Soc.* **2010**, *132*, 3248−3249. (g) Macfarlane, R. J.; Lee, B.; Jones, M. R.; Harris, N.; Schatz, G. C.; Mirkin, C. A. *Science* **2011**, *334*, 204−208. (h) Tan, S. J.; Campolongo, M. J.; Luo, D.; Cheng, W. *Nat. Nanotechnol.* **2011**, *6*, 268−276. (i) Xu, L.; Ma, W.; Wang, L.; Xu, C.; Kuang, H.; Kotov, N. A. *Chem. Soc. Rev.* **2013**, *42*, 3114−3126.

(2) (a) Mirkin, C. A.; Letsinger, R. L.; Mucic, R. C.; Storhoff, J. J. *Nature* **1996**, *382*, 607−609. (b) Katz, E.; Willner, I. *Angew. Chem., Int. Ed.* **2004**, *43*, 6042−6108. (c) Lu, Y.; Liu, J. *Acc. Chem. Res.* **2007**, *40*, 315−323. (d) Tikhomirov, G.; Hoogland, S.; Lee, P. E.; Fischer, A.; Sargent, E. H.; Kelley, S. O. *Nat. Nanotechnol.* **2011**, *6*, 485−490. (e) Xing, H.; Wong, N. Y.; Xiang, Y.; Lu, Y. *Curr. Opin. Chem. Biol.* **2012**, *16*, 429−435.

(3) (a) Suzuki, K.; Hosokawa, K.; Maeda, M. *J. Am. Chem. Soc.* **2009**, *131*, 7518−7519. (b) Hu, S.-H.; Gao, X. *J. Am. Chem. Soc.* **2010**, *132*, 7234−7237. (c) Du, J.; O'Reilly, R. K. *Chem. Soc. Rev.* **2011**, *40*, 2402−2416. (d) Zhang, S.; Li, Z.; Samarajeewa, S.; Sun, G.; Yang, C.; Wooley, K. L. *J. Am. Chem. Soc.* **2011**, *133*, 11046−11049. (e) Wang, Y.; Wang, Y.; Breed, D. R.; Manoharan, V. N.; Feng, L.; Hollingsworth, A. D.; Weck, M.; Pine, D. J. *Nature* **2012**, *491*, 51−55.

(4) Xu, L.; Kuang, H.; Xu, C.; Ma, W.; Wang, L.; Kotov, N. A. *J. Am. Chem. Soc.* **2011**, *134*, 1699−1709.

(5) (a) Xu, X.; Rosi, N. L.; Wang, Y.; Huo, F.; Mirkin, C. A. *J. Am. Chem. Soc.* **2006**, *128*, 9286−9287. (b) Sardar, R.; Heap, T. B.; Shumaker-Parry, J. S. *J. Am. Chem. Soc.* **2007**, *129*, 5356−5357. (c) Claridge, S. A.; Liang, H. W.; Basu, S. R.; Fréchet, J. M. J.; Alivisatos, A. P. *Nano Lett.* **2008**, *8*, 1202−1206. (d) Mastroianni, A. J.; Claridge, S. A.; Alivisatos, A. P. *J. Am. Chem. Soc.* **2009**, *131*, 8455−8459. (e) Maye, M. M.; Nykypanchuk, D.; Cuisinier, M.; van der Lelie, D.; Gang, O. *Nat. Mater.* **2009**, *8*, 388−391. (f) Fan, Z.; Govorov, A. O. *Nano Lett.* **2010**, *10*, 2580−2587. (g) Yan, W.; Xu, L.; Xu, C.; Ma, W.; Kuang, H.; Wang, L.; Kotov, N. A. *J. Am. Chem. Soc.* **2012**, *134*, 15114−15121. (h) Yoon, J. H.; Lim, J.; Yoon, S. *ACS Nano* **2012**, *6*, 7199−7208.

(6) Gansel, J. K.; Thiel, M.; Rill, M. S.; Decker, M.; Bade, K.; Saile, V.; von Freymann, G.; Linden, S.; Wegener, M. *Science* **2009**, *325*, 1513−1515.

(7) Zhang, S.; Park, Y.-S.; Li, J.; Lu, X.; Zhang, W.; Zhang, X. *Phys. Rev. Lett.* **2009**, *102*, 023901.

(8) Hentschel, M.; Schäferling, M.; Weiss, T.; Liu, N.; Giessen, H. *Nano Lett.* **2012**, *12*, 2542−2547.

(9) Hendry, E.; Carpy, T.; Johnston, J.; Popland, M.; Mikhaylovskiy, R. V.; Lapthorn, A. J.; Kelly, S. M.; Barron, L. D.; Gadegaard, N.; Kadodwala, M. *Nat. Nanotechnol.* **2010**, *5*, 783−787.

(10) (a) Perro, A.; Reculusa, S.; Ravaine, S.; Bourgeat-Lami, E.; Duguet, E. *J. Mater. Chem.* **2005**, *15*, 3745−3760. (b) Jiang, S.; Chen, Q.; Tripathy, M.; Luijten, E.; Schweizer, K. S.; Granick, S. *Adv. Mater.* **2010**, *22*, 1060−1071. (c) Lee, J.-H.; Kim, G.-H.; Nam, J.-M. *J. Am. Chem. Soc.* **2012**, *134*, 5456−5459.

(11) (a) Ohnuma, A.; Cho, E. C.; Camargo, P. H. C.; Au, L.; Ohtani, B.; Xia, Y. *J. Am. Chem. Soc.* **2009**, *131*, 1352−1353. (b) Chen, T.; Chen, G.; Xing, S.; Wu, T.; Chen, H. *Chem. Mater.* **2010**, *22*, 3826−3828. (c) Li, Z.; Cheng, E.; Huang, W.; Zhang, T.; Yang, Z.; Liu, D.; Tang, Z. *J. Am. Chem. Soc.* **2011**, *133*, 15284−15287. (d) Gröschel, A. H.; Walther, A.; Löbling, T. I.; Schmelz, J.; Hanisch, A.; Schmalz, H.; Müller, A. H. E. *J. Am. Chem. Soc.* **2012**, *134*, 13850−13860. (e) He, J.; Perez, M. T.; Zhang, P.; Liu, Y.; Babu, T.; Gong, J.; Nie, Z. *J. Am. Chem. Soc.* **2012**, *134*, 3639−3642.

(12) (a) Worden, J. G.; Shaffer, A. W.; Huo, Q. *Chem. Commun.* **2004**, 518−519. (b) Sung, K.-M.; Mosley, D. W.; Peelle, B. R.; Zhang, S.; Jacobson, J. M. *J. Am. Chem. Soc.* **2004**, *126*, 5064−5065. (c) Xing, H.; Wang, Z.; Xu, Z.; Wong, N. Y.; Xiang, Y.; Liu, G. L.; Lu, Y. *ACS Nano* **2011**, *6*, 802−809.

(13) Chen, T.; Yang, M.; Wang, X.; Tan, L. H.; Chen, H. *J. Am. Chem. Soc.* **2008**, *130*, 11858−11859.

(14) Wang, H.; Chen, L.; Feng, Y.; Chen, H. *Acc. Chem. Res.* **2013**, *46*, 1636−1646.

(15) Zhang, X.; Servos, M. R.; Liu, J. *J. Am. Chem. Soc.* **2012**, *134*, 7266−7269.

(16) Hill, H. D.; Millstone, J. E.; Banholzer, M. J.; Mirkin, C. A. *ACS Nano* **2009**, *3*, 418−424.

(17) Elghanian, R.; Storhoff, J. J.; Mucic, R. C.; Letsinger, R. L.; Mirkin, C. A. *Science* **1997**, *277*, 1078−1081.

(18) Liu, J.; Lu, Y. *J. Am. Chem. Soc.* **2003**, *125*, 6642−6643.

(19) In Figure 4b, the quenching of the fluorescence signal was observed to be incomplete. Since the a-(D1+D4)-AuNP were washed via centrifugation at least 5 times and the fluorescence signal of the supernatant solution was found to be insignificant and similar to that of the buffer solution, we conclude that the fluorescent signal is not due to free FAM-DNA as 5 times of centrifugation should also be able to remove free polymer micelles which are small (Alemdaroglu, F. E.; Alemdaroglu, N. C.; Langguth, P.; Herrmann, A. *Adv. Mater.* **2008**, *20*, 899−902). Since the quenching efficiency of AuNP is known to be highly distance dependent (Reineck, P.; Gómez, D.; Ng, S. H.; Karg, M.; Bell, T.; Mulvaney, P.; Bach, U. *ACS Nano* **2013**, *7*, 6636−6648), the incomplete quenching of the fluorescence signal is a result of relatively long distance between the fluorophore and the AuNPs.

(20) Chen, Q.; Whitmer, J. K.; Jiang, S.; Bae, S. C.; Luijten, E.; Granick, S. *Science* **2011**, *331*, 199−202.

(21) (a) Verma, A.; Uzun, O.; Hu, Y.; Hu, Y.; Han, H.-S.; Watson, N.; Chen, S.; Irvine, D. J.; Stellacci, F. *Nat. Mater.* **2008**, *7*, 588−595. (b) Wu, L. Y.; Ross, B. M.; Hong, S.; Lee, L. P. *Small* **2010**, *6*, 503−507. (c) Walther, A.; Müller, A. H. E. *Chem. Rev.* **2013**, *113*, 5194−5261.